

# Microstructures associated with stress relaxation around indentations in Y and Nd based melt textured ceramic superconductors

A. PROULT

*Laboratoire de Métallurgie Physique, UMR 6630-CNRS, Université de Poitiers-UFR Sciences SP2MI, Bd Marie et Pierre Curie, BP 30179, 86962 Futuroscope Chasseneuil Cedex, France*  
E-mail: anne.proult@univ-poitiers.fr

P. D. TALL

*Département de Physique, Faculté des Sciences et Techniques, Université Cheikh Anta Diop, Dakar, Sénégal*

J. RABIER

*Laboratoire de Métallurgie Physique, UMR 6630-CNRS, Université de Poitiers-UFR Sciences SP2MI, Bd Marie et Pierre Curie, BP 30179, 86962 Futuroscope Chasseneuil Cedex, France*

Microstructures associated with room temperature indentation subsequently annealed at 450°C have been analyzed by TEM in Y and Nd based melt textured ceramic superconductors. It is shown that stress relaxation around indentations occurs by the nucleation of stacking faults with  $\mathbf{R} = 1/6\langle 031 \rangle$  displacement vector in Y based material. Differently relaxation occurs in NdBaCuO by the nucleation of perfect dislocations with  $\langle 100 \rangle$  Burgers vectors which can be locally dissociated. A model is proposed to explain these microstructures and is related to the difference in energies of stacking faults with  $\mathbf{R} = 1/6\langle 031 \rangle$  displacement vector in these compounds.

© 2001 Kluwer Academic Publishers

## 1. Introduction

The high level of the critical current density  $J_c$ , which is essential for large-scale applications of high  $T_c$  superconductor ceramics, is strongly dependent on the pinning of the vortices. Therefore it is of great interest to introduce flux pinning centers to these materials. As high  $T_c$  superconductors are characterised by a coherence length of the same order as the interatomic distances [1], lattice defects are liable to act as pinning centers: stacking faults, vacancies, twin planes. . . Dislocations are potential pinning centers of this kind and can act through strain effects as well as stoichiometric effects [2, 3]. Vortex pinning by dislocations has been clearly demonstrated in the case of low-angle grain boundary [4]. In this context, thermomechanical treatments can be used to create a defect microstructure optimising the flux pinning.

High  $T_c$   $\text{YBa}_2\text{Cu}_3\text{O}_{7-x}$  (Y123) superconductors exhibit a complex microstructure: twin planes, stacking faults, dislocations, precipitates of second phase  $\text{Y}_2\text{BaCuO}_5$  (Y211). These defects are created during the high temperature processing or by thermomechanical treatments. The stacking faults are due to the intercalation of a CuO plane in the matrix Y123, followed by a shear  $\mathbf{b}/2$ , leading to the formation of a  $(\text{CuO})_2$  double layer [5]. The unit cell created locally by this intercalation corresponds to that of the  $\text{YBa}_2\text{Cu}_4\text{O}_8$

(Y248) compound (space group Ammm, orthorhombic cell,  $a = 3.86 \text{ \AA}$   $b = 3.86 \text{ \AA}$   $c = 27.24 \text{ \AA}$ ) [6]. At room temperature, the matrix Y123 is unstable and can decompose to form the Y248 compound which is stable below 800°C. As a consequence of this phase transformation, the stacking fault energy appear to be negative [7]. These stacking faults, lying in the (001) plane, decrease the  $c$ -axis correlation length of vortices leading to a lower activation energy for the vortices movement [8].

Because of the anisotropic structure of Y123, the dislocations are observed essentially in the (001) plane [9] that corresponds to the calculated stable configuration [10]. When the applied field is parallel to the  $c$ -axis, these linear defects act as punctual pinning centers.

High  $T_c$   $\text{NdBa}_2\text{Cu}_3\text{O}_{7-x}$  (Nd123) superconductor represents an interesting alternative material. Its structure is similar to that of Y123, however, as the Nd ionic radius is close to the Ba ionic radius, a substitution takes place between Nd and Ba sites to form a solid solution. The Nd123 structure is then less anisotropic than the Y123 one. As a matter of fact, the Nd123 microstructure was less investigated than the Y123 microstructure. Nevertheless Sandiumenge *et al.* [11] previously reported the observation of dislocations out of the (001) plane aligned along or close to the [001] direction in melt-textured Nd123. On the contrary as dislocations

lying in the (001) plane, such dislocations can act as correlated linear pinning centers when the applied field is parallel to the [001] axis.

Since high  $T_c$ , sharp transition and large values of  $J_c$  have been observed in oxygen control melt growth NdBaCuO [12], it is well known that the Nd system can exhibit superior properties compared to the Y system. High values of  $J_c$  were also observed in NdBaCuO material prepared in air [13] and superior properties of Nd over Y thin films were obtained [14].

Owing to the brittleness of these materials, deformations at room temperature can only be achieved by microindentation or by deformation under a confining pressure. This paper reports on transmission electron microscopy (TEM) observations of deformation microstructures around indentations performed in Y and Nd based melt-textured ceramics.  $YBa_2Cu_3O_{7-x}$  materials containing respectively 30 %wt of  $Y_2BaCuO_5$  (Y211), and 20 %wt Y211 and  $NdBa_2Cu_3O_{7-x}$  containing 15 %wt of  $Nd_4Ba_2Cu_2O_{10}$  (Nd422) were investigated. The Nd422 phase, called the brown phase, corresponds in the Nd system to the Y211 green phase of the Y phase system.

## 2. Experimental set up

The samples, grown by melt-textured processing, contain large single domains [15]. They were indented at room temperature perpendicularly to the basal plane (001) (load 5 g, dwell time 5 s). They were then annealed in air for three hours at 450°C in order to promote plastic deformation over larger areas away from the indentation site. The TEM thin foils were mechanically polished down to 50  $\mu\text{m}$  and ion milled at the nitrogen temperature at 4 kV and 0.5 mA on the non-indented face during 7 hours, then at 3 kV and 0.3 mA on both faces for 2 hours. TEM observations were performed on a Jeol 200 CX microscope operating at 200 kV.

## 3. Results

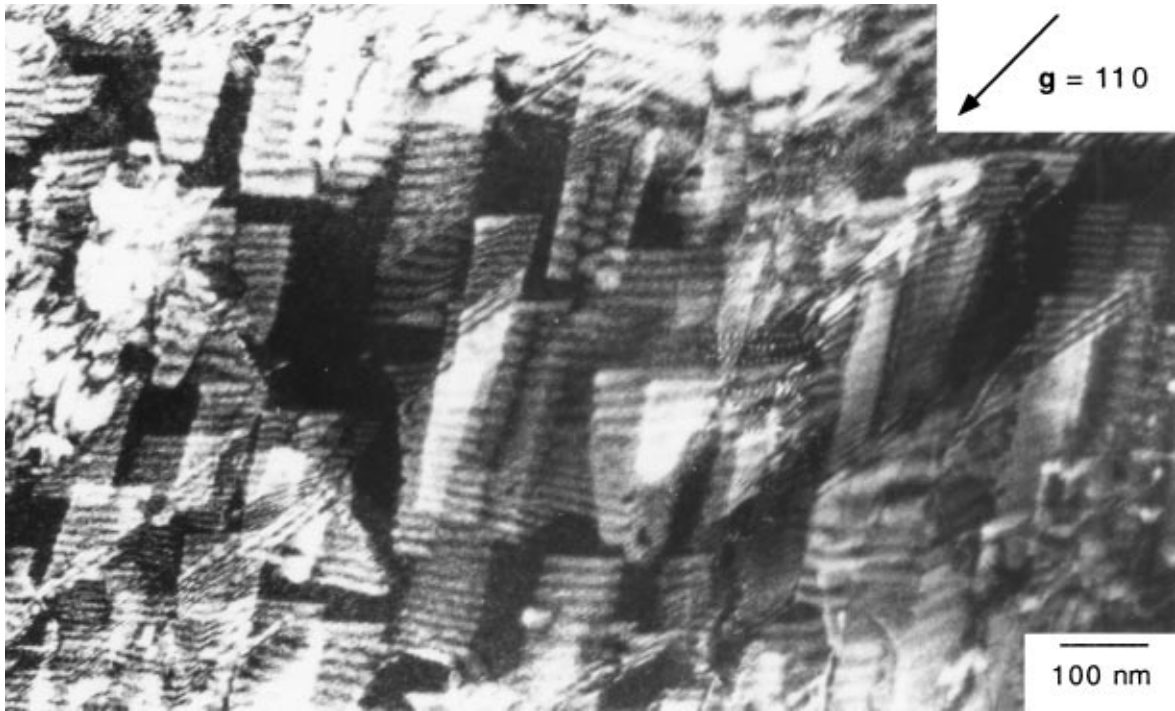
### 3.1. Y123-30 %wt Y211

Fig. 1a shows the microstructure observed in Y123-30 %wt Y211 after indentation at room temperature and subsequent annealing. It is characterised by a high density of stacking faults that are not solely confined to the vicinity of the indentation. Their density is homogeneous in the whole sample whereas no perfect dislocation was observed. Since the as-grown material shows a very low density of defects, with the exception of the mirror twin structure, it can be assumed that stacking faults observed in figure 1a are due to the thermo-mechanical treatment. These stacking faults lie in the (001) plane and are elongated along the [100] direction. The contrasts obtained with different diffraction vectors ( $\mathbf{g} = 400$ ,  $\mathbf{g} = 0\bar{1}3$ ,  $\mathbf{g} = 110$ ,  $\mathbf{g} = \bar{1}10$ ,  $\mathbf{g} = \bar{1}13$ ) are consistent with the fault vector  $\mathbf{R} = 1/6[031]$  which is one of the classical fault vectors  $\mathbf{R} = 1/6(031)$  observed in Y123. We do not observe any evidence of interaction between these stacking faults and Y211 inclusions. On the weak beam image (Fig. 1b) obtained with  $\mathbf{g} = 220$ , the diffraction conditions are such that the

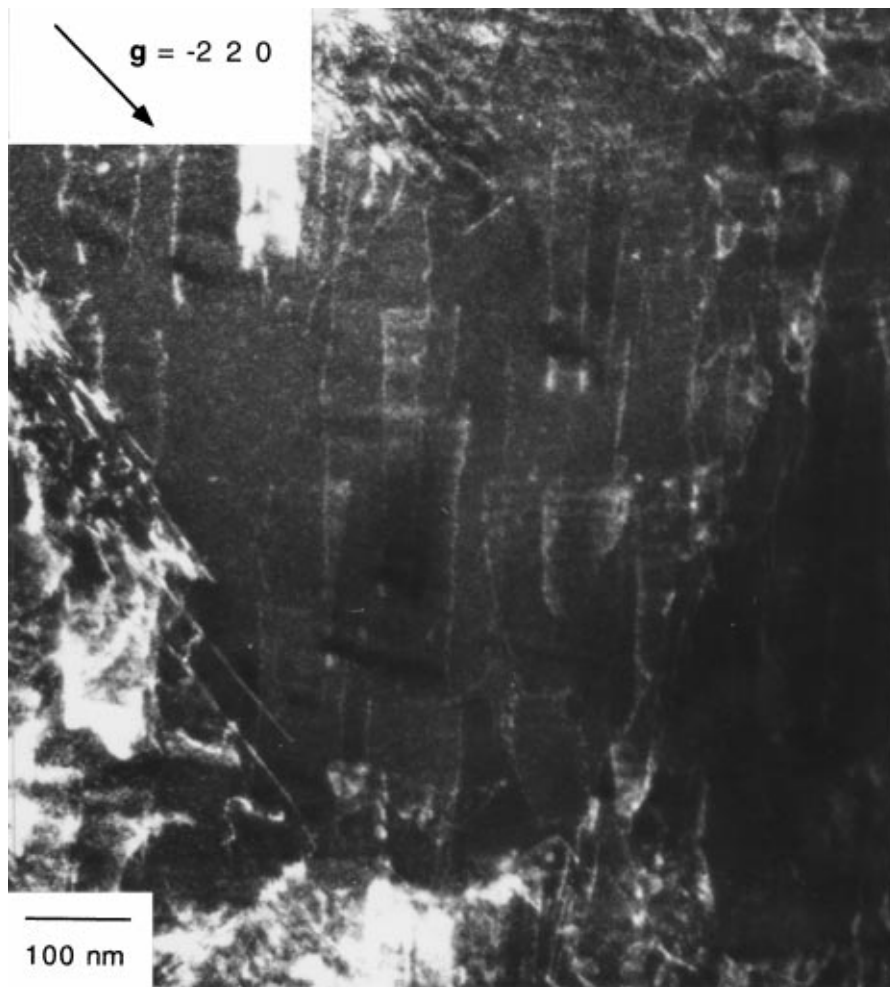
faults are out of contrast. The faults appear as bounded by partial dislocations. However, the density of faults as well as the density of dislocations is too high to clearly associate a single fault to one pair of partial dislocations. It has been shown that in YBaCuO, a stacking fault characterised by a fault vector  $\mathbf{R} = 1/6(031)$  can result from different mechanisms: a  $\mathbf{R} = 1/6[031]$  stacking fault is limited by two partial dislocations with Burgers vectors  $1/6[031]$  and  $1/6[03\bar{1}]$  when it results from the precipitation of CuO onto a perfect dislocation or by a unique dislocation loop with Burgers vector  $\mathbf{b} = 1/6[031]$  when it results from CuO precipitation in the bulk of the material [7]. In order to discriminate between these two possible configurations, the diffraction vector  $\mathbf{g} = 0\bar{1}3$  can be used. Indeed, if imaging with such a diffraction vector, stacking faults with displacement vector  $\mathbf{R} = 1/6[031]$  will be out of contrast as well as dislocations characterised by a Burgers vector  $\mathbf{b} = 1/6[031]$ ; differently dislocations with  $\mathbf{b} = 1/6[03\bar{1}]$  Burgers vectors will be in contrast. In figure 1c, which has been obtained with such a diffraction vector ( $\mathbf{g} = 0\bar{1}3$ ), dislocations are visible but their density is much lower than on figure 1b, implying that dislocations with  $\mathbf{b} = 1/6[03\bar{1}]$  Burger vector exist in much smaller density. According to these observations, it can be deduced that two families of dislocations are associated with the occurrence of stacking faults with  $\mathbf{R} = 1/6[031]$ , i.e. a large density of dislocations with  $\mathbf{b} = 1/6[031]$  Burgers vector and a small density of dislocations with  $\mathbf{b} = 1/6[03\bar{1}]$  Burgers vector. This microstructure is consistent with the fact that a large number of stacking faults are nucleated within the bulk of the material rather than nucleated on perfect dislocations.

### 3.2. Y123-20 %wt Y211

Fig. 2a was obtained for Y123-20 %wt Y211, in the vicinity of the indentation. It shows two families of elongated stacking faults lying in the (001) plane, their direction being [100] or [010]. The contrasts observed with different diffracting vectors ( $\mathbf{g} = 200$ ,  $\mathbf{g} = 020$ ,  $\mathbf{g} = 1\bar{1}0$ ,  $\mathbf{g} = 110$ ,  $\mathbf{g} = 10\bar{3}$ ,  $\mathbf{g} = 0\bar{1}\bar{3}$ ,  $\mathbf{g} = 0\bar{1}3$ ,  $\mathbf{g} = \bar{3}03$ ) are consistent with a fault vector  $\mathbf{R} = 1/6[301]$ . These configurations are analogous to usual observations of these defects which are elongated along the in plane screw characters of the bounding dislocations, i.e.  $1/6[301]$  and  $1/6[031]$ . However in the present case, these configurations are not so simple as far as bounding partial dislocations are concerned. Indeed in figure 2b, which has been obtained with the diffracting vector  $\mathbf{g} = 200$ , these stacking faults are consistently out of contrast, but the bounding dislocations of the two types of stacking faults are in contrast whereas partials with  $1/6[031]$  Burgers vector should have been out of contrast. Furthermore these bounding dislocations show further dissociations, those dissociations being different in the different twin variants (see dislocations (A) and (B)). Different dissociations depending of the crystal variant have already been reported and discussed [16]. However the dislocation substructures observed here appear to be more complex and have not been

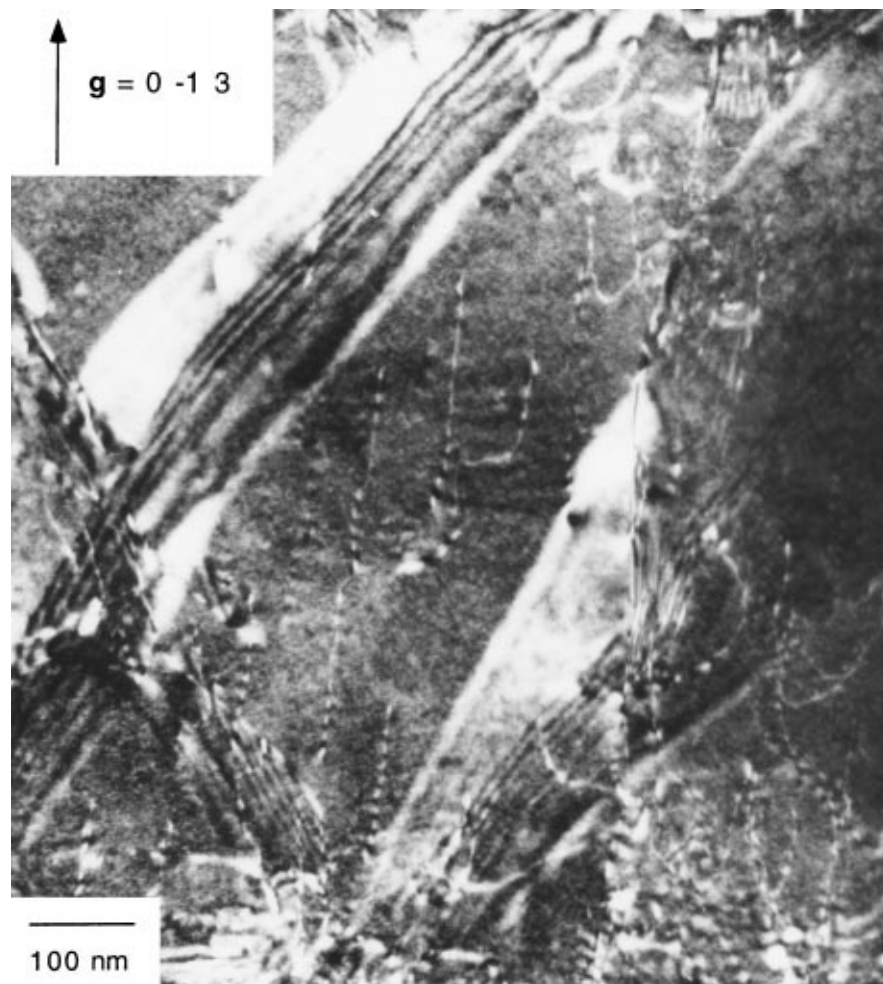


(a)



(b)

Figure 1 Microstructure of YBaCuO-30 wt% Y211 indented at room temperature and annealed at 450°C. Large density of stacking faults lies in (001) plane. (a) : weak beam dark field obtained with  $\mathbf{g} = 110$ , the stacking faults lie along the [100] direction. (b) : weak beam dark field obtained with  $\mathbf{g} = \bar{2}20$ . The stacking faults are out of contrast. Bounding dislocations are in contrast. (c) : weak beam dark field obtained with  $\mathbf{g} = 0\bar{1}3$ . Stacking faults and most of dislocations are out of contrast. Few dislocations are still in contrast. (Continued)



(c)

Figure 1 (Continued).

reported before in YBCO. They are not fully understood. These contrasts could be explained by the superposition of different planar faults in parallel planes as well as by multiple interactions between bounding dislocations. Investigations are still in progress. However it is worth noting that stacking fault nucleation appears to be the main stress relaxation process near indentations. Indeed other dislocations (C) which exhibit different features than (A) and (B) dislocations are also in evidence. These perfect dislocations are parallel to  $\langle 110 \rangle$  and  $[010]$  directions. Such dislocations were also observed in the matrix between indentations so that they appear as as-grown defects and are not related to the plastic deformation mechanisms induced by indentations.

### 3.3. Nd123-15 %wt Nd422

Compared to preceding materials, the indented Nd123 exhibits a low density of defects confined to the vicinity of indentations. Fig. 3 shows typical features of the deformation substructure which is built with straight dislocations. Such dislocation straightness can be related to a high Peierls potential or to an elastic anisotropy of the material. This last point can not be checked out since elastic constants are not known. All these dislocations are perfect dislocations characterised by a Burger vector

$\mathbf{b} = [100]$  and lie along the  $\langle 110 \rangle$  directions parallel to mirror twin boundaries. Although those dislocations are seen undissociated on most of their lengths, white arrows in Fig. 3 point out a few dissociations. Such dissociations occur when the dislocations change their direction, for instance from direction  $[110]$  to  $[\bar{1}10]$ , and are very localised.

No wide extended stacking faults are observed in the deformed area and no interaction between twin structure and dislocations was in evidence.

## 4. Discussion

Indentation at room temperature creates a very high density of dislocations confined to a small volume in the vicinity of indentation. Then, it generates locally an important stress field. The subsequent heat treatment induces an increase of the plastic zone size and stresses can then be relaxed in two ways: by motion of the dislocations created during indentation at room temperature or/and by nucleation of new defects.

### 4.1. Comparison between Y123-30 wt% Y211 and Y123-20 wt% Y211:

In both micro-indented materials, a very high density of stacking faults is observed. It is now established that

these stacking faults correspond to the intercalation of a CuO layer, in the Y123 matrix, parallel to the (001) plane [5, 17]. Rabier *et al.* [7] have shown that perfect dislocations with  $\langle 100 \rangle$  Burger vector increase the thermodynamical range of nucleation of the CuO layer: the CuO plane can then precipitate in the core of a pre-existing dislocation that dissociates into two partials bounding the stacking fault:

$$\langle 100 \rangle \rightarrow 1/6\langle 30\bar{1} \rangle + 1/6\langle 301 \rangle$$

Perfect dislocations act then as favourable sites for formation of stacking faults.

Actually, both observed microstructures do not fit with this theory: in YBaCuO-30 wt Y211, each stacking fault with fault vector  $\mathbf{R} = 1/6\langle 301 \rangle$  is limited by a unique partial dislocation loop with a Burger vector  $\mathbf{b} = 1/6\langle 031 \rangle$  and in YBaCuO-20 wt Y211, although the nature of the bounding partials is difficult to sort out, stacking faults geometries are clearly related to the precipitation of CuO within the matrix.

Fig. 4 presents a possible interpretation of the observed microstructure obtained after indentation in YBaCuO: indentation at room temperature generates a large density of dislocations in the close vicinity. During the heat treatment at 450°C, extra CuO planes



(a)

*Figure 2* Microstructure of YBaCuO-20 wt Y211 indented at room temperature and annealed at 450°C. (a) : weak beam dark field obtained with  $\mathbf{g} = 110$ , two families of stacking faults are in contrast as well as dislocations. Stacking faults lie along  $[100]$  or  $[010]$  directions. (b) : weak beam dark field obtained with  $\mathbf{g} = 200$ . Stacking faults are out of contrast. Three families (A, B and C) of dislocations are in contrast. Note the contrast associated to the twin mirror boundaries. A and B are partial dislocations bounding the two types of stacking faults. Black arrows indicate dissociation of A dislocations. C dislocations are perfect dislocations. (*Continued*)



(b)

Figure 2 (Continued).

can precipitate on these dislocations, before they can glide and multiply. Then Frank Read sources cannot operate anymore since dislocations are made sessile by CuO precipitation (dislocations 'dissociate' following the reaction  $\langle 100 \rangle \rightarrow 1/6\langle 30\bar{1} \rangle + 1/6\langle 301 \rangle$  leading to partials dislocations with a Burger vector component out of the glide plane) so that dislocations are locked in the vicinity of indentations. In order to relax the remaining stress, extra CuO planes can precipitate on germination sites in the matrix. As a consequence most of the stresses are relaxed in YBaCuO by planar defects in the matrix and not by dislocations.

Comparing YBaCuO-30 %wt Y211 and YBaCuO-20 %wt Y211, we notice that the density of these extra planes drastically increases when the density of Y211 phase increases. Sandiumenge *et al.* reported that a high density of Y211 inclusions and especially of Y211/Y123 interfaces enhances the CuO planes pre-

cipitation [18]. Such interfaces could act as preferential diffusion paths requisite for the growth of an extra CuO plane. Y211 precipitates could also act as degraded regions with lower copper concentration, balancing local copper enrichment of Y123 matrix by CuO plane inclusions. Although we do not notice interactions between stacking faults and Y211 precipitates, our observations support the idea that the planar defects formation is enhanced by a high density of Y211 inclusions.

As far as superconducting properties are concerned, such a high density of stacking faults can be detrimental. Indeed when the magnetic field is applied parallel to the *c*-axis, the stacking faults lead to a segmentation of vortices [8]: the *c*-axis correlation length of the flux line lattice is reduced and the irreversibility line is shifted toward lower fields and temperatures. On the other hand, partial dislocations limiting the stacking faults act as punctual pinning centres and allow

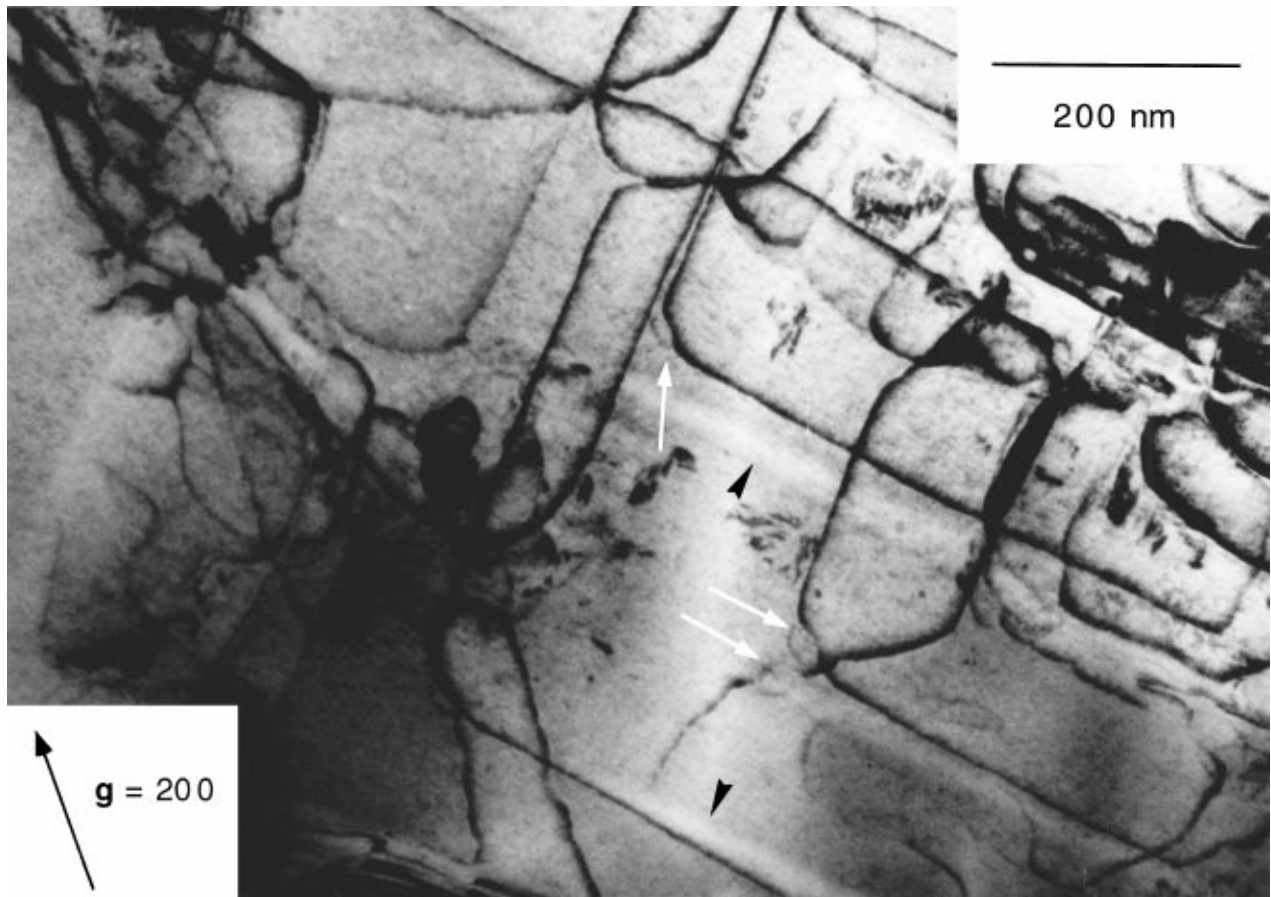


Figure 3 Microstructure of NdBaCuO-15 wt Nd422 indented at room temperature and annealed at 450°C. Bright field image obtained with  $g = 200$ . Perfect dislocations are in contrast. White arrows show local dissociations. Twins mirror are also in contrast (black arrows).

for an increase in the critical current density  $J_c$ . It has been shown that the relevant parameter is then the ratio “dislocation length/fault surface” [11]. In both indented Y123 ceramics, which exhibit a strong density of stacking faults, this criterion is not optimised.

#### 4.2. Comparison between Nd123-15 wt% Nd422 and Y123-20 wt% Y211:

Unlike Y123 ceramics, Nd123 ceramics form a  $Nd_{1+y}Ba_{2-y}Cu_3O_{7-x}$  solid solution: the structure is then less anisotropic and we can expect a more 3-dimensional dislocation substructure to be obtained after plastic deformation than in Y123. One aim of this work on Nd123 was then to create dislocations out of the basic (001) plane. It would allow for an increase of the pinning of vortices when the applied field is parallel to  $c$ -axis. According to our TEM observations, it has been proved to be impossible to create such dislocations out of (001) plane by the plastic deformation process reported here.

However, defects introduced by plastic deformation in Nd123 and in Y123 show very different characteristics. All dislocations observed in Nd123 in the vicinity of the indentation are perfect dislocations whereas all dislocations observed in Y123 are partial dislocation loops limiting a stacking fault. Strain relaxation mechanisms are then completely different in  $YBa_2Cu_3O_{7-x}$  materials than in  $NdBa_2Cu_3O_{7-x}$ , although their structure is quite similar. In Y123, the strain seems to be

relaxed by nucleation of CuO planes in the matrix, whereas in Nd123, perfect dislocations control the plastic deformation. A relaxation mechanism in NdBaCuO ceramics is proposed in Fig. 5: as in YBaCuO ceramics, dislocations in NdBaCuO are generated at room temperature close to the indentations. But in NdBaCO, precipitation of CuO planes on dislocations cores during the annealing procedure seem to be less efficient: perfect dislocations can glide and multiply in (001) plane during the heat treatment. The strain in the matrix is then relaxed by nucleation of perfect dislocations. Only few precipitations of CuO planes on these dislocations cores one time dislocations have move away from the indentation site.

In Y system, Y211 inclusions promote the stacking faults nucleation [18]. Assuming that the same phenomenon occurs in Nd system, then the difference of secondary phase concentration between both materials (20 wt% of Y211 in Y123 and 15 wt% of Nd422 in Nd123) is unable to explain the difference in stacking fault concentrations observed in both materials. Rather, the energy associated with the stacking fault formation seems to be much larger in Nd123 than in Y123. Indeed in the Nd compound, these faults are confined on strong curvatures of dislocations lines: solely when the line energy is important, does dislocation dissociation becomes energetically favourable.

In Y123, stacking faults are described as germs of the Y248 phase. This latter phase was already obtained as thin films [6] as well as bulk materials [19]. Although

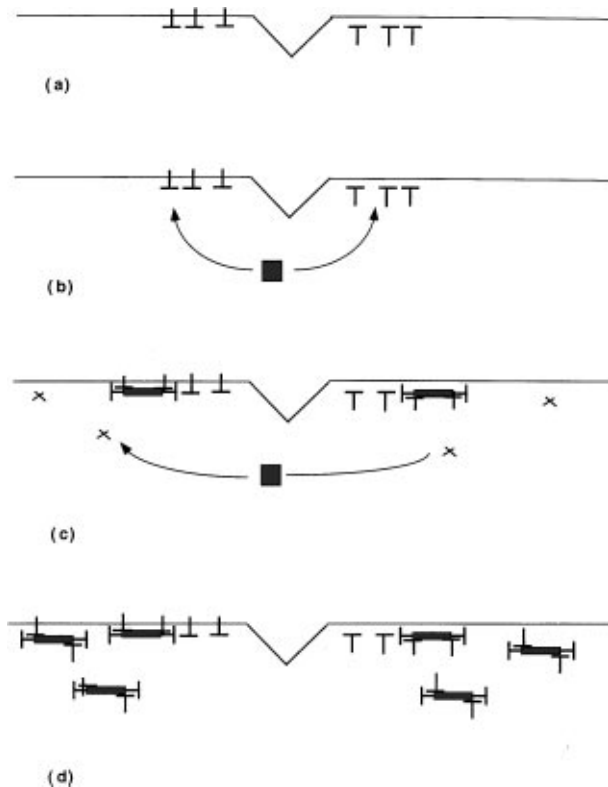


**Figure 4** Mechanism for relaxation of strain induced by indentation in YBaCuO ceramics. (a) : indentation at room temperature generates a large amount of dislocations confined in a small volume near the indentation. (b) : during the heat treatment, CuO planes precipitate into cores of dislocations before they glide or multiply. (c) : Frank-Read sources operation is impeded by non glissile dislocations : precipitation of CuO plane on dislocation with  $[100]$  Burger vector yield to a 'dissociated' dislocation  $[100] \rightarrow 1/6[30\bar{1}] + 1/6[301]$ . (d) : precipitation of CuO planes in the matrix on germination sites yielding to additional CuO planes surrounded by partial dislocation loops with  $1/6(031)$  Burger vector. The stress is relaxed by precipitation of CuO planes in the matrix after annealing.

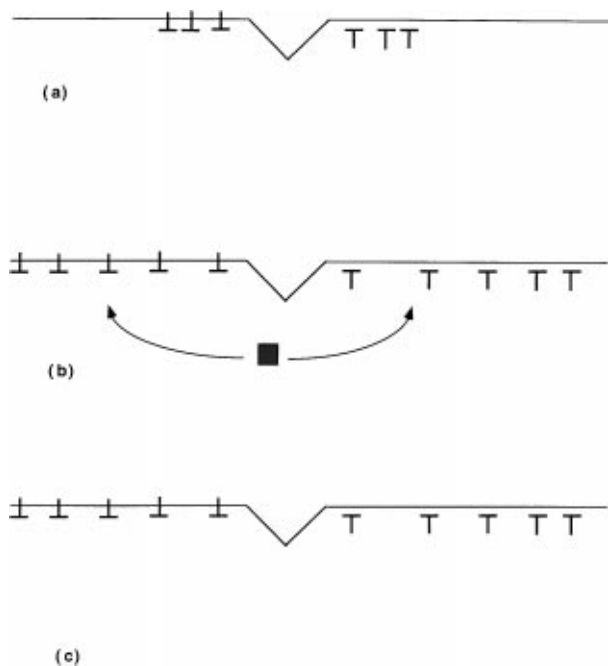


**Figure 5** Mechanism for relaxation of strain induced by indentation in NdBaCuO ceramics. (a) : indentation at room temperature generates a large amount of dislocations confined in a small volume near the indentation. (b) : during the annealing treatment, glide and multiplication of dislocations is not impeded by CuO precipitation and take place in (001).

TEM observations of stacking faults in as-grown directionally solidified NdBaCuO superconductors have already been reported [11], no corresponding phase in the Nd-Ba-Cu-O system phase diagram was observed [20]. This is consistent with the hypothesis that stacking faults have a larger energy than in Y systems.

## 5. Conclusion

Stress relaxation processes after indentation at room temperature and subsequent annealing in YBCO and NdBCO systems have proved to be very different. In Y compounds this is mainly achieved through the nucleation of stacking faults with  $1/6\langle 301 \rangle$  displacement vectors and by perfect dislocations with  $\langle 100 \rangle$  Burgers vectors in Nd compound. This is consistent with at higher stacking fault energy in NdBCO compared to Y compounds. Indeed, when CuO precipitation on dislocations is possible this prevents the movement and multiplication of dislocations away from the indentation site and stress relaxation occurs by CuO precipitation within the matrix. This is observed in Y compounds. Although dislocations resulting from stress relaxation were observed in NdBCO, none of them were found to lie out of the (001) plane as was expected from structural features. This method does not allow to evidence defects that could act as linear and therefore more efficient pinning centers : perfect dislocations observed in micro-indented Nd123 lie in the (001) plane and are likely to act as punctual pinning centers when the applied field is parallel to the  $c$ -axis. However, the fact that it is possible to generate dislocations and only a small amount of stacking fault surfaces in this material seems promising. Under these conditions, the pinning efficiency of dislocations should not be balanced by the detrimental effect of the planar defects.

## Acknowledgements

The authors thank Dr S. Pinol (ICMAB Barcelona-Spain) for providing the melt textured YBaCuO samples and Dr R. Yu (ICMAB Barcelona-Spain) for providing the melt textured NdBaCuO samples.

## References

1. W. J. GALLAGHER, T. K. WORTHINGTON, T. R. RINGER, F. HOLTZBERG, D. L. KAISER and R. L. SANDSTROM, *Physica B* **148** (1987) 221.
2. R. J. CAVA, B. BATLOGG, S. A. SUNSHINE, T. SIEGRIST, R. M. FLEMING, K. RABE, L. F. SHNEEMYER, D. W. MURPHY, R. B. VANDOVER, P. K. GALLAGHER, S. H. GLARUM, S. NAKAHARA, R. C. FARROW, J. J. KRAJEWSKI, S. M. ZAHURAK, J. V. WASZCZAK, J. H. MARSHALL, P. MARSH, L. W. RUPP, W. F. PECK and E. A. RIETMAN, *Physica C* **153-155** (1988) 560.
3. V. SELVAMANIKAM, M. MIRONOVA, S. SON and K. SALAMA, *ibid.* **208** (1993) 238.
4. A. DIAZ, L. MECHIN, P. BERGHUIS and J. E. EVETTS, *Phys. Rev. Lett.* **80** (1998) 3855.
5. H. W. ZANDBERGEN, R. GRONSKY, K. WANG and G. THOMAS, *Nature* **331** (1988) 596.
6. P. MARSH, R. M. FLEMING, M. L. MANDLICH, A. M. DESANTO, J. KWO, M. HONG and L. J. MARTINEZ-MIRANDA, *ibid.* **334** (1988) 141.



7. J. RABIER, P. D. TALL and M. F. DENANOT, *Phil Mag A* **67** (1993) 1021.
8. N. VIVALTA, F. SANDIUMENGE, E. RODRIGUEZ, B. MARTINEZ, S. PINOL, X. OBRADORS and J. RABIER, *Phil Mag B* **75** (1997) 431.
9. J. RABIER and M. F. DENANOT, *Journal of Less-Common Metals* **164 & 165** (1990) 223.
10. J. RABIER, in "Plastic Deformation of Ceramics," edited by R. C. Bradt *et al.* (Plenum Press, New York, 1995).
11. F. SANDIUMENGE, N. VIVALTA, J. RABIER and X. OBRADORS, *Appl. Phys. Lett.* **73**(18) (1998) 2660.
12. J. G. YOO, C. Y. HUANG, Y. Y. XUE, C. W. CHU, X. W. CAO and J. C. HO, *Phys. Rev. B* **51** (1995) 12900.
13. H. KOJO, S. I. YOO and M. MURAKAMI, *Physica C* **289** (1997) 85.
14. M. BADAYE, J. G. WEN, F. FUKUSHIMA, N. KOSHIZUKA, T. MORISHITA, N. NISHIMURA and Y. KIDO, *Supercond. Sci. Tech.* **10** (1997) 825.
15. S. PINOL, V. GOMIS, F. SANDIUMENGE, B. MARTINEZ, A. LABARTA, J. FONTCUBERTA and X. OBRADORS, *J. Alloys Compounds* **195** (1993) 11.
16. J. RABIER and M. F. DENANOT, *Phil. Mag. A* **65** (1992) 427.
17. G. VAN TENDELOO, H. W. ZANDBERGEN, J. VAN LANDUYT and S. AMELINCKX, *Material Characterization* **27** (1991) 59.
18. F. SANDIUMENGE, N. VIVALTA, S. PINOL, B. MARTINEZ and X. OBRADORS, *Phys. Rev. B* **51 n°10** (1995) 6645.
19. B. DABROWSKI *Supercond. Sci. Technol.* **11** (1998) 54.
20. S. I. YOO and R. W. MAC CALLUM, *Physica C* **210** (1993) 147.

*Received 1 June  
and accepted 13 November 2000*